A Positive Role of microRNA-15b on Regulation of Osteoblast Differentiation

S. Vimalraj[1], **Nicola C. Partridge**[2], and **N. Selvamurugan**[1,*]

[1]Department of Biotechnology, School of Bioengineering, SRM University, Kattankulathur 603 203, Tamil Nadu, India

[2]Department of Basic and Craniofacial Biology, New York University College of Dentistry, New York, NY 10010, USA

Abstract

Osteoblast differentiation is tightly regulated by several factors including microRNAs (miRNAs). In this paper we report that pre-mir-15b is highly expressed in differentiated osteoblasts. The functional role of miR-15b in osteoblast differentiation was determined using miR-15b mimic/ inhibitor and the expression of osteoblast differentiation marker genes such as alkaline phosphatase (ALP), type I collagen genes was decreased by miR-15b inhibitor. Runx2, a bone specific transcription factor is generally required for expression of osteoblast differentiation marker genes and in response to miR-15b inhibitor treatment, Runx2 mRNA expression was not changed; whereas its protein expression was decreased. Even though Smurf1 (SMAD specific E3 ubiquitin protein ligase 1), HDAC4 (histone deacetylase 4), Smad7, and Crim1 were found to be few of miR-15b's putative target genes, there was increased expression of only Smurf1 gene at mRNA and protein levels by miR-15b inhibitor. miR-15b mimic treatment significantly increased and decreased expressions of Runx2 and Smurf1 proteins, respectively. We further identified that the Smurf1 3'UTR is directly targeted by miR-15b using the luciferase reporter gene system. This is well documented that Smurf1 interacts with Runx2 and degrades it by proteasomal pathway. Hence, based on our results we suggest that miR-15b promotes osteoblast differentiation by indirectly protecting Runx2 protein from Smurf1 mediated degradation. Thus, this study identified that miR-15b can act as a positive regulator for osteoblast differentiation.

Keywords

Osteoblasts; miR-15b; Smurf1; Runx2; Mesenchymal stem cells; HDAC4

Introduction

Mesenchymal stem cells (MSCs) have the potential to undergo self-renewal and multilineage differentiation including osteoblastic lineage. The existence of an osteoblast is committed through the cascade of osteoprogenitors and pre-osteoblasts; each step is tightly

*To whom correspondence should be made: Nagarajan Selvamurugan, Ph. D., Professor, Department of Biotechnology, School of Bioengineering, SRM University, Kattankulathur 603 203. Tamil Nadu. India. Cell: 91-9940632335, selvamurugan.n@ktr.srmuniv.ac.in, selvamn2@yahoo.com.

regulated by various types of growth factors, cytokines, signaling molecules, hormones, morphogens etc (Chen et al., 2012; Liu et al., 2013; Raggatt et al., 2008; Monroe et al., 2012; Selvamurugan et al., 2000). Any kind of modification or deficiency in these regulators may lead to pathological effects. Runx2 is one of the major transcription factors for the osteoblast differentiation and it activates osteoblast differentiation marker genes. Its expression and activation are controlled by several signaling pathways including BMP (Bone Morphogenetic Protein)/TGF-β (Transforming Growth Factor-β) signaling pathways. In BMP/TGF-β signaling pathway, the cellular actions involve specific type-1 and type-2 (serine-threonine kinase) receptor complex and intracellular signaling through phosphorylation of specific regulatory Smads (R-Smads; Smad-1,2,3,5,8). The activated regulatory Smads form a complex with Smad-4 (common Smad) and translocate to the nucleus for gene activation (Chen et al., 2012; Selvamurugan et al., 2007). The BMP signaling increases Runx2 and alkaline phosphatase (ALP) expression and the increased Runx2 expression suppress myogenesis with the help of Smads induced ALP expression (Raggatt et al., 2008; Lee at al., 2000 Jensen at al., 2009). Smads and Runx2 play indispensable role in osteoblast differentiation. SMAD specific E3 ubiquitin protein ligase 1 (Smurf1), a HECT domain E3 ubiquitin ligase mediates degradation of Runx2, type1 BMP receptor and BMP activated Smad1 and smad5 proteins (Zhao et al., 2004; Murakami et al., 2003; Zhu et al., 1999).

MicroRNAs (miRNAs) are endogenously expressing non-coding RNAs (~25 nt) that regulate gene expression by targeting 3' untranslated region (UTR) of mRNAs at posttranscriptional level. Recent evidence shows that miRNAs play a significant role in diverged physiological process, including cell growth, apoptosis, development, metabolism, stress adaptation, hormone signaling, proliferation and differentiation. During skeletal development, several miRNAs have been identified as positive (miR-20a, 210, 27, 29c, 196a) and negative (miR-138, 204, 211, 133, 135) regulators (Lian et al., 2012; Vimalraj and Selvamurugan, 2012; Moorthi et al., 2013; Vimalraj et al., 2013). Therefore, miRNAs are considered to be a closely related regulator of osteogenesis and bone formation.

Even though expression of several miRNAs has been reported to be MSC or osteoblast specific, their functional role during osteoblast differentiation is not yet completely determined. For instance, microarray profiling and real time PCR analysis of miR-15b expression during osteoblast differentiation has been reported in previous studies (Guo et al., 2009; Nishi et al., 2010; Gao et al., 2011), but no evidence of its functional regulation on osteoblast differentiation has been documented to date. In this study, we investigated pre-mir-15b expression and identified it as osteoblast differentiation related miRNA. To determine the functional role of miR-15b in osteoblast differentiation, transient transfections with miR-15b inhibitor/mimic, followed by real time RT-PCR and Western blot analyses were carried out in human, mouse and rat osteoblastic cells. Our results show that inhibition of miR-15b leads to decreased osteoblast differentiation at molecular and cellular levels. Most importantly, miR-15b inhibitor decreased expression of Runx2 protein expression and that could be due to increased expression of Smurf1 protein during osteoblast differentiation. Increased expression of Runx2 protein was found by miR-15b mimic and that could be due to decreased expression of Smurf1 protein during osteoblast differentiation.

Materials and Methods

Cell culture and osteo differentiation

Human bone marrow stromal cells (hBMSCs) was isolated from 27 years old female and cultured according to previously described method (Pittenger et al., 1999). The Institutional review committee in SRM University approved the protocol for isolation of hMSCs. They were obtained with the written consent from donor. Adult rat dissection and osteoprogenitor cells isolation from calvaria of 2 day old rat pups were followed as described previously (Nefussi et al., 1985). All animal procedures were approved by the University of Madras and SRM university animal ethical committees. The primary hBMSCs and rat osteoprogenitor cells were induced to osteo differentiation in osteogenic medium [alpha MEM (Cellgro), 15% FBS (Fetal Bovine Serum), Penicillin-Streptomycin (Invitrogen), 10^{-4} M L-Ascorbic Acid, 10^{-8} M Dexamethasone and 1.80 mM Potassium phosphate monobasic (Sigma)]. The medium was changed once in three days.

Transient transfection

The cells were seeded in 6-well plates with 1×10^5 cells/2 ml growth medium per well on the day before the transfection. miR-15b inhibitor (Applied Biosystems: MH10904) designed to bind with endogenous miR-15b, when introduced into cells, inhibits their activities. miR-15b mimic (Applied Biosystems: MC10904) was designed to similar to that of endogenous miR-15b. These were studied with a negative control miRNA (Applied Biosystems: 4464076). The transfection reagent (X-treme Gene transfection reagent from Roche, USA) was mixed with 50 nM of miR-15b inhibitor or negative control miRNA, and transient transfection was carried out according to the manufacturer's protocol. Rat osteoblasts and human osteoblastic cells (MG63) or mouse MSCs, (C3H10T1/2) were allowed 7 days for differentiation; whereas human MSCs were allowed 10 days for differentiation.

Real-time RT-PCR analysis

Total RNA was isolated from cultured cells with Trizol reagent (Invitrogen) according to the manufacturer's instructions and quantitative estimation done by Qubit 2.0 Flurometer (Invitrogen). cDNA was synthesised using GeNei AMV RT-PCR kit, according to the manufactures's protocol as follows: 2 μg of total RNA, 1μl of oligo(dT)18/ random hexamer (50μM) and 1μl of dNTP Mixture (10mM) were added and made upto 14μl reverse transcript reaction solution using RNase free water, followed by incubation at 65° C for 5 mins and subjected to fast chill using ice cubes. Then 4μl of 5X First-strand Buffer, 1μl of Reverse Transcriptase (200U/μl) and 1μl of RNase Inhibitor (40U/μl) were added to 14μl reverse transcript reaction solution and this reaction mixture was kept in 30° C for 10 min, 42° C for 50 min and 95 °C for 5 min in thermal cycler. The real-time PCR analysis was performed in Bio-Rad system using Kapa sybr fast qPCR kits (Kapa Biosystem) according to the manufacturer's instruction. The primers for stem loop sequence of miR-15b and other genes used in this study are given in Table 1. The Ct (threshold cycle) values were calculated from amplification curve.   Ct value of a gene was calculated by subtracting the Ct value of internal control gene from the Ct value of that gene. The   Ct value was calculated by subtracting the   Ct value of control with the   Ct value of treated and then the

Ct values were converted to fold change by raising 2 to the   Ct power. The thermal cycling conditions were as follows: 95° C for 5 mins as initial denaturation, followed by 40 cycles of 95° C for 30s, 58° C for 30s and 72° C for 30s, with a final extension at 72° C for 5 mins.

Western Blot Analysis

Cells were washed with cold phosphate buffered saline (PBS), and solubilized in lysis buffer (RIPA buffer- Sigma-Aldrich, Product Number R 0278; 50 mM Tris-HCl, pH 8.0, with 150 mM sodium chloride, 1.0% Igepal CA-630 (NP-40), 0.5% sodium deoxycholate, and 0.1% sodium dodecyl sulfate) containing a protease inhibitor mixture (Sigma-Aldrich, Cat #P8340) (AEBSF-[4-(2-Aminoethyl) benzenesulfonyl fluoride hydrochloride], Aprotinin, Bestatin hydrochloride, E-64 - [N-(trans-Epoxysuccinyl)-L-leucine 4-guanidinobutylamide], Leupeptin hemisulfate salt, Pepstatin A). The Cell lysates were centrifuged at 10000 rpm for 10 min at 4° C and supernatant was transferred into fresh tube followed by estimation of total proteins by Qubit 2.0 Flurometer (Invitrogen). 20 ug of protein was loaded per well and separated on a 12% polyacrylamide gel, followed by transfer into a nitrocellulose membrane (Bio-Rad) by electroblotting. 5% non fat milk powder was used to block the nonspecific binding site in the membrane and incubated with primary antibody for overnight at 4° C. Then the membrane was probed with secondary antibody conjugated with horseradish peroxidase. Finally the bands were visualized by adding SuperSignal West Dura Extended Duration Substrate (Thermo scientific) according to the manufacturer's instructions. The obtained images were quantified by subjecting to ImageJ software (http://rsbweb.nih.gov/ij/) as described previously (Hartig et al., 2013). A monoclonal Smurf1 antibody from Santa Cruz Biotechnology and a polyclonal Smurf1 antibody from Abcam were used in this study. The mouse monoclonal antibody Runx2 (1:1000), HDAC4 (1:1000), CDK2 (1:1000) and α-tubulin (1:1000) antibodies and the secondary antibodies conjugated with horseradish peroxidase (HRP) were obtained from Santa Cruz Biotechnology.

Mineralized matrix formation analysis

Osteoblast mineralized matrix was determined by alizarin red staining. Briefly, at the end of transfection period, cells were washed twice with ice-cold PBS and fixed for 1 hr with 10% formalin at room temperature. It was then rehydrated with 1 ml of distilled water for 5 min. The cells were stained with 1% alizarin red in 2% ethanol (pH 4.0) for 5 mins at room temperature followed by rinsing with deionized water and incubated in PBS for 15 min to remove nonspecific staining. The stained matrix was documented as bright red color by inverted light microscope (Magnus). The staining was quantified by adding 10% acetic acid and heated at 85°C for 10 min, and subsequently kept on ice for 5 min. The acid was neutralized by adding Ammonium hydroxide; red color was obtained then quantified by spectrophotometry at 405 nm.

Alkaline phosphatase activity

Cells were washed with PBS and then fixed with 10% formalin for 20 min, followed by 1 min fixation in pre chilled ethanol and acetone (50:50), and then again washed with PBS. The preparation of ALP solution was done by mixing of 1 mg of Naphthol AS-MX (Sigma-Aldrich, Cat # N4875) in one droplet of N, N-dimethylformamide (Sigma-Aldrich, Cat #

D4551) and the mixture was dissolved in 10 ml of 0.1 M Tris-HCl buffer (pH 8.5) containing 2 mM MgCl$_2$. 6 mg of Fast Blue BB salt (Sigma-Aldrich, Cat # F3378) was added to the above solution and filtered. The ALP solution was added to the fixed cells and incubated at 37°C for 20 min, and p-Nitrophenyl phosphate, 4mg/ml (SRL, Cat # 144816) was added and read the plate at 405 nm using Synergy HT multimode microplate reader (Bio-Tek, USA).

Luciferase reporter assay

The wild 3' UTR of Smurf1 (sense: 5' AAACTAGCGGCCGCCTTGTTTTGAAGTATTGCTGCTAT 3', antisense: 3' TTTGATCGCCGGCGGAACAAAACTTCATAACGACGATAGATC 5') and mutant 3' UTR of Smurf1 (sense: 5' AAACTAGCGGCCGCCTTGTTTTGAAGTATTGAAGCTAT 3', antisense: 3' TTTGATCGCCGGCGGAACAAAACTTCATAACTTCGATAGATC 5') were chemically synthesized. These sense and antisense primers of either wild or mutant Smurf1 containing an internal NotI site were annealed and cloned between PmeI and XbaI restriction sites present in pmirGLO dual-luciferase miRNA target expression vector (Cat# E1330; Promega, USA). The Smurf1 NCBI Reference Sequence ID is NM_020429. The clones containing Smurf1 3'UTR sequence were identified by NotI digestion. C3H10T1/2 cells were transiently transfected with 50 nM of miR-15b mimic, miR-15b inhibitor or negative control miRNA along with 200 ng of the wild or mutant Smurf1 3'UTR constructs using Lipofectamine 2000 transfection reagent (Invitrogen, Cat# 11668-027). After 24 hr of transfection, cells were harvested with passive lysis buffer (PLB) and the luciferase activity was measured in Synergy HT multimode microplate reader (Bio-Tek) using dual luciferase reporter assay system (Promega, Cat# E1910). Firefly luciferase activity was normalized to *Renilla* luciferase activity and all experiments were performed in triplicates.

Bioinformatics target prediction

We identified miR-15bs' putative targets using the following computational algorithms, TargetScan 6.2 (http://www.targetscan.org/), PicTar (http://pictar.mdc-berlin.de/), TarBase (http://diana.cslab.ece.ntua.gr/tarbase/), miRanda (http://www.microrna.org/microrna/home.do) and miRecords (http://mirecords.umn.edu/miRecords/). miRmap and PITA were used to quantify the thermodynamic stability of miR-15b-mRNA duplex. The miRmap identifies thermodynamic energy, probabilistic, evolutionary and sequence information on the interaction between miRNA-target sites. This calculates the MFE (Minimum Free Energy) of TG duplex. The binding energy (TG binding) is computed based on ensemble free energy. TG duplex seed is the measurement of MFE of the seed with RNAcofold and TG binding seed is the binding energy of the seed based on ensemble free energy. TG open is referred to mRNA opening free energy-accessibility, in other words it is calculating the energy required to unfold the target site of 3'-UTR. TG total is calculated by sum of TG duplex with TG open (TG total= TG duplex + TG open). Raw data of miRmap scores for each feature, e.g. 'TG total' represents in kcal/mol. Probability (binomial/exact distribution) determines the expected probability of an exact seed match or full miRNA binding site of target. The conservation is identified as branch length score (BLS) on 3'UTR fitted tree and PhyloP, SPH (Siepel, Pollard and Haussler) test from PhyloP program. miRmap score represents the predicted miRNA target repression strength (http://mirmap.ezlab.org/)

(Vejnar Zdobnov, 2012; Vejnar et al., 2013). In addition, PITA (Probability of Interaction by Target Accessibility), a thermodynamic modeling program provides the energy scores of microRNA-target interactions. It is used to calculate TG duplex, TG open and TG total. TG total (TTG) is equal to the difference between TG duplex and TG open. TG open is referred to the energy required to make the target region open for miRNA binding and TG duplex is referred to the binding free energy of miRNA and target duplex structure. PITA settings were 6 minimal seed size, 0 minimum seed conservation, and no flank (http://genie.weizmann.ac.il/index.html) (Kertesz et al., 2007; Wilmink et al., 2010).

Statistical analysis

The statistical analysis was carried out using one way ANOVA. The significant difference ($P < 0.05$) between groups was determined by the student's *t*-test. All data were shown as mean ± standard deviation (SD) with n=3.

Results and Discussion

Identification of pre-mir-15b expression during osteoblast differentiation

Several miRNAs have been reported to be a key regulator of osteoblast differentiation at various levels (Vimalraj and Selvamurugan, 2012; Moorthi et al., 2013). Even though a number of miRNAs have been identified, only few miRNAs have been validated for their functional role during osteoblast differentiation. In this study our aim was to determine the expression and the functional role of miR-15b during MSCs differentiation into osteoblasts. To determine the distribution of pre-mir-15b expression *in vivo*, total RNA was isolated from different types of tissues of adult rats and was subjected to real time RT-PCR analysis. The tissues included were of bone, muscle, adipose, skin, heart, liver, kidney and lung. The result showed that there is differential expression of pre-mir-15b among the different rat organs (Fig. 1A). pre-mir-15b expression was significantly down regulated in muscle, kidney, skin and was up regulated in heart, lung. There was no change in pre-mir-15b expression in adipose and liver compared to bone tissue (Fig. 1A). In general, pre-mir-15b was found to be expressed in all tissues analyzed. Differential expression of miR-15b in different types of normal human tissues has also been reported by others (Guo et al., 2009; Nishi et al., 2010; Gao et al., 2011). We next examined whether the expression of pre-mir-15b can be regulated during MSCs differentiation into osteoblasts. MSCs can differentiate into osteoblastic cells when appropriate internal and external conditions are provided. Fig. 1B represents the expression of pre-mir-15b during differentiation of osteoblasts that included undifferentiated human MSCs (hMSCs), 7 days osteo differentiated hMSCs, 14 days osteo differentiated hMSCs, differentiated human osteoblasts (MG63) and rat osteoprogenitor cells. The result (Fig. 1B) showed that the expression of pre-mir-15b is found to be 2–3 fold increased during osteo differentiation of hMSCs compared to undifferentiated hMSCs. In this study we determined the expression level of precursor mir-15b not the mature miR-15b. It has been reported that in primary effusion lymphoma, the levels of mature form correlates with the levels of precursor form in more than 60% of miRNAs documented (O'Hara et al., 2008). However, oHhthe levels of mature miRNAs could change from the levels of precursor miRNAs due to the process of transportation and maturation based on the cellular context.

The potential role of miR-15b has been documented in miRecords which showed that 5 genes from human and 2 genes from rat have been targeted by miR-15b [in human, Bcl-2 (B-cell CLL/lymphoma 2), RECK (reversion-inducing-cysteine-rich protein with kazal motifs), CCNE1 (cyclin E1), MKK4 (MAPK (mitogen-activated protein kinase) kinase 4) and BMI1 (B lymphoma Mo-MLV insertion region 1 homolog) and in rat, Bcl-2 (B-cell CLL/lymphoma 2) and Arl2 (ADP ribosylation factor-like 2)]. Furthermore, the role of miR-15b has been studied in various cancerous cells (Satzger et al., 2010; Liu et al., 2012) and myocardial infarction (Nishi et al., 2010; Liu et al., 2012). Since pre-mir-15b expression is relatively high in differentiated osteoblasts from our study (Fig. 1B), this suggested that miR-15b can act as a positive regulator for osteoblast differentiation.

Functional role of miR-15b in osteoblast differentiation

We next analyzed the functional role of miR-15b during osteoblast differentiation by performing a series of experiments. Rat osteoprogenitor cells were transiently transfected with either negative control or miR-15b inhibitor. The transfected osteoprogenitor cells were cultured upto 7 days in normal and osteogenic medium followed by RNA isolation and real time RT-PCR analysis for osteoblast differentiation marker genes such as alkaline phosphatase (ALP), type I collagen. When cells transfected with negative control or miR-15b inhibitor in the presence of normal medium, there was no change in mRNA expression of ALP and type I collagen (Fig. 2A). When cells were transiently transfected with miR-15b inhibitor in the presence of osteogenic medium, mRNA expression of ALP and type I collagen was decreased (Fig. 2A). ALP and type 1 collagen are early osteoblast differentiation markers genes (Gutierrez et al., 2002; Jensen et al., 2009; Monroe et al., 2012; Wang et al., 2013). To further confirm these findings, C3H10T1/2 cells were transfected with negative control or miR-15b inhibitor in the presence of osteogenic medium. After 7 days, cells were subjected to quantification of ALP activity and mineralized matrix formation by alizarin red staining. We found that transfection of miR-15b inhibitor into C3H10T1/2 cells significantly reduced ALP activity (Fig. 2B) as well as formation of mineralized bone matrix (Figs. 2C and 2D). To determine the effects of miR-15b on differentiated osteoblasts, MG63 cells were transiently transfected with either negative control or miR-15b inhibitor in the presence of osteogenic medium. After 7 days, cells were stained with alizarin red and quantification of alizarin red was carried out. Inhibition of miR-15b significantly decreased matrix mineralization compared to the cells transfected with negative control miRNA (Figs. 2E and 2F). Thus, these results from MSCs, osteoprogenitor and differentiated osteoblasts (Fig. 2) suggested that miR-15b has a positive role during osteoblast differentiation.

miR-15b regulates Runx2 protein expression

Most of the osteoblast differentiation marker genes require Runx2, a bone specific transcription factor (Ducy et al., 1997; Komori et al., 1997; Banerjee et al., 1997). It is also evident that miR-15b regulates expression of ALP and type I collagen followed by matrix mineralization (Fig. 2). Hence, we examined whether expression of Runx2 gene can be regulated by miR-15b. In order to determine whether miR-15b targets Runx2, hMSCs were transiently transfected with either negative control or miR-15b inhibitor, followed by RNA isolation and real time RT-PCR analysis. The result showed that there is no change in

expression of Runx2 mRNA in response to miR-15b inhibitor under either normal medium or osteogenic medium (Fig. 3A). It is expected because Runx2 was not identified as a direct target gene of miR-15b by bioinformatics tools. Since expression of osteoblast differentiation marker genes and osteoblast mineralization were regulated by miR-15b (Fig. 2), and Runx2 activity can be altered by the post translational mechanisms such as acetylation, ubiquitination, phosphorylation, protein-protein interactions (Jeon et al., 2006; Wang et al., 2013; Boumah et al., 2009; McGee-Lawrence et al., 2013; Lengner et al., 2005), we determined Runx2 protein expression. Human MSCs were transiently transfected with either negative control or miR-15b inhibitor and were allowed to differentiate them. Whole cell lysates were prepared and subjected to Western blot analysis. The result indicates that the expression of Runx2 protein was decreased when cells were transiently transfected with miR-15 inhibitor (Figs. 3A and 3B).

In silico investigation and validation of miR-15b's target genes

Since a single miRNA can target up to hundreds of mRNAs, finding its target genes is an important step to understand its regulatory network. In this regard, the *in silico* analyses were used initially to narrow down to find the functional importance of miR-15b targets towards osteogenic commitments. The putative targets of miR-15b can be classified according to their negative contribution in osteogenic differentiation or positive contribution to other lineages using online softwares. Among them some key regulators or antagonistic effectors of osteogenesis such as Smad7, Smurf1, Crim1, HDAC4, HOXC8, TGIF2 were included and these genes were well documented their antagonistic role in osteogenesis (Jeon et al., 2006; Chen et al., 2012; He at al., 2012, Moorthi et al., 2013). The 3'UTR regions of Crim1, HDAC4, Smad7 and Smurf1 hold at least 6-nt perfect complementarities to the miR-15b seed region. According to TargetScan and miRanda target prediction, the interspecies conservation of putative miR-15b target sites within the Smurf1, Smad7, Crim1 and HDAC4 3′-UTR are shown in Figs. 4A–D. The shadow or colored pointed sequences indicate the perfectly conserved sequences between human and other species. To identify potential interactions between miR-15b and its targets based on thermodynamic stability, we used miRmap and PITA algorithm. These algorithms provide the information on the energy obtained when miRNA-mRNA duplex formed, and higher negative TG duplex values may represent potential repression. Among the target genes, Smurf1 3'UTR has more negative miRmap score indicating its more vulnerability to miR-15b (Table 2). However, several studies demonstrated negative regulation of osteoblast differentiation by Crim1, Smad7, HDAC4 and Smurf1 (Jeon et al., 2006; Chen et al., 2012; Monroe et al., 2012; He at al., 2012). To validate these putative target genes of miR-15b, rat osteoprogenitor cells were transiently transfected with either negative control or miR-15b inhibitor and were allowed to differentiate. To determine the expression level of these target genes, total RNA was isolated, followed by real time RT-PCR analysis. There was no change in mRNA expression of Crim1 and Smad7; whereas there was a significant increase of Smurf1 mRNA by miR-15b inhibitor (Fig. 4E). However, the possibility of miR-15b induced repression and reduced protein synthesis of Crim1 and SMAD7 proteins during osteoblast differentiation cannot be ruled out.

miR-15b targets Smurf1 protein

Smurf1 was identified as a target gene for miR-15b (Fig. 4A) and it mediates degradation of Runx2 by ubiquitination pathway and its overexpression decreases BMP signaling (Zhao et al., 2004; Jensen et al., 2009). BMP2 acetylates Runx2 by p300 to protect from Smurf1 mediated degradation of Runx2. HDAC4 and 5 are the proteins involved in deacetylation of Runx2 followed by smurf1 mediated degradation (Westendorf et al., 2002; Jeon et al., 2006; Boumah et al., 2009). It has been shown that Smad6 binds with Runx2 and subjects to Smurf1 mediated degradation (Shen et al., 2006). Furthermore, Smurf1 has been reported to target JunB (Zhao et al., 2010), BMP/TGF-β type 1 receptor, Smad1 and Smad5, (Murakami et al., 2003; Zhu et al., 1999; Kavsak et al., 2000; Zhao et al., 2004) and mediates ubiquitination pathway followed by degradation. It is well documented that Runx2 interacts with several cofactors (Westendorf et al., 2002; Selvamurugan et al., 2006; Niger et al., 2013). Its activity can be altered by its interacting proteins and/or the posttranslational modifications (Yang et al., 2011; Wang et al., 2013). Since we already identified that miR-15b targets Smurf1 (Fig. 4E) and it is evident that Smurf1 degrades Runx2 protein by interacting with it, followed by ubiquitination and proteasomal pathway (Satzger et al., 2010; Liu et al., 2012), we next determined expression of Smurf1 protein. Human MSCs were transiently transfected with either negative control or miR-15b inhibitor and were allowed to differentiate. Whole cell lysates were prepared and subjected to Western blot analysis. The result indicates that there was increased expression of Smurf1 proteins when cells were transiently transfected with miR-15 inhibitor (Figs. 5A and 5B); whereas there was no change in expression of HDAC4 protein (Figs. 5C and 5D), which is also a target of miR-15b and a negative regulator of Runx2 transcriptional activity (Jeon et al., 2006; Boumah et al., 2009; Shimizu et al., 2010; McGee-Lawrence et al., 2011). In addition to human MSCs, mouse MSCs (C3H10T1/2) were also transiently transfected with either control miRNA or miR-15b inhibitor/miR-15b mimic. After 7 days, whole cell lysates were prepared and subjected to Western blot analysis for Smurf1 and Runx2 proteins. The results showed that the expression of Runx2 protein was significantly increased by miR-15b mimic whereas it was significantly decreased by miR-15b inhibitor. However, the expression of Smurf1 protein was significantly decreased by miR-15b mimic but it was significantly increased by miR-15b inhibitor (Figs. 6A and 6B). We also determined the mRNA expression levels of Runx2 and Smurf1 after miR-15b inhibitor treatment in these cells. The result indicated that there was no significant change in Runx2 mRNA expression whereas Smurf1 mRNA level was significantly increased (Fig. 6C). Collectively, our results suggest that miR-15b can promote osteoblast differentiation by targeting of Smurf1 and inhibition of degradation of Runx2.

Luciferase analysis

To determine whether miR-15b directly targets Smurf1 3'UTR, a dual luciferase reporter assay system was used. *Renilla* luciferase gene present in pmirGLO construct is constitutively active and its activity can be used for normalization of firefly luciferase activity. The pmirGLO construct or the pmirGLO construct containing either the wild or mutant Smurf1 3'UTR downstream to the firefly luciferase reporter gene were transiently co-transfected along with miR-15b mimic, miR-15b inhibitor or negative control miRNA

into C3H10T1/2 cells. The pmirGLO construct had no change in luciferase activity in response to miR-15b mimic, inhibitor or negative control treatments (Fig. 7). Similarly, the pmirGLO construct containing the mutant Smurf1 3'UTR had no change in luciferase activity in response to miR-15b mimic, inhibitor or negative control treatments; whereas the pmirGLO construct containing the wild Smurf1 3'UTR had significantly reduced luciferase activity by miR-15b mimic treatment compared to negative control (Fig. 7). Thus, this result suggested that miR-15b can directly target the 3'UTR of the Smurf1 gene.

Overall, our study suggests that miR-15b expression might play an essential role during osteoblast differentiation by targeting the gene (Smurf1) which is involved in antagonistic functions of osteoblast function. Additionally, other putative targets of miR-15b (HDAC4, Smad7 and Crim1) were analyzed and there was no change in their expression. It appears that miR-15b promotes osteoblast differentiation by directly targeting Smurf1 and indirectly protecting Runx2 protein. In conclusion, this study identified that miR-15b can act as a positive regulator for osteoblast differentiation.

Acknowledgments

Literature Cited

Banerjee C, McCabe LR, Choi JY, Hiebert SW, Stein JL, Stein GS, Lian JB. Runt homology domain proteins in osteoblast differentiation: AML3/CBFA1 is a major component of a bone-specific complex. J Cell Biochem. 1997; 66:1–8. [PubMed: 9215522]

Boumah CE, Lee M, Selvamurugan N, Shimizu E, Partridge NC. Runx2 recruits p300 to mediate parathyroid hormone's effects on histone acetylation and transcriptional activation of the matrix metalloproteinase-13 gene. Mol Endocrinol. 2009; 23:1255–1263. [PubMed: 19423655]

Chen G, Deng C, Li YP. TGF-β and BMP signaling in osteoblast differentiation and bone formation. Int J Biol Sci. 2012; 8:272–288. [PubMed: 22298955]

Ducy P, Zhang R, Geoffroy V, Ridall AL, Karsenty G. Osf2/Cbfa1: a transcriptional activator of osteoblast differentiation. Cell. 89:747–754. [PubMed: 9182762]

Gao J, Yang T, Han J, Yan K, Qiu X, Zhou Y, Fan Q, Ma B. MicroRNA expression during osteogenic differentiation of human multipotent mesenchymal stromal cells from bone marrow. J Cell Biochem. 2011; 112:1844–1856. [PubMed: 21416501]

Guo CJ, Pan Q, Li DG, Sun H, Liu BW. miR-15b and miR-16 are implicated in activation of the rat hepatic stellate cell: An essential role for apoptosis. J Hepatol. 2009; 50:766–778. [PubMed: 19232449]

Gutierrez S, Javed A, Tennant DK, van Rees M, Montecino M, Stein GS, Stein JL, Lian JB. CCAAT/ enhancer-binding proteins (C/EBP) beta and delta activate osteocalcin gene transcription and synergize with Runx2 at the C/EBP element to regulate bone-specific expression. J Biol Chem. 2002; 277:1316–1323. [PubMed: 11668178]

Hartig SM. Basic image analysis and manipulation in ImageJ. Curr Protoc Mol Biol. 2013

He L, Yang N, Isales CM, Shi XM. Glucocorticoid-induced leucine zipper (GILZ) antagonizes TNF-α inhibition of mesenchymal stem cell osteogenic differentiation. PLoS One. 2012; 7:e31717. [PubMed: 22396737]

Jensen ED, Gopalakrishnan R, Westendorf JJ. Bone morphogenic protein 2 activates protein kinase D to regulate histone deacetylase 7 localization and repression of Runx2. J Biol Chem. 2009; 284:2225–2234. [PubMed: 19029091]

Jeon EJ, Lee KY, Choi NS, Lee MH, Kim HN, Jin YH, Ryoo HM, Choi JY, Yoshida M, Nishino N, Oh BC, Lee KS, Lee YH, Bae SC. Bone morphogenetic protein-2 stimulates Runx2 acetylation. J Biol Chem. 281:16502–16511. [PubMed: 16613856]

Kaimal V, Bardes EE, Tabar SC, Jegga AG, Aronow BJ. ToppCluster: a multiple gene list feature analyzer for comparative enrichment clustering and network-based dissection of biological systems. Nucleic Acids Res. 2010; 38(Web Server issue):W96–W102. [PubMed: 20484371]

Kavsak P, Rasmussen RK, Causing CG, Bonni S, Zhu H, Thomsen GH, Wrana JL. Smad7 binds to Smurf2 to form an E3 ubiquitin ligase that targets the TGF beta receptor for degradation. Mol Cell. 2000; 6:1365–1375. [PubMed: 11163210]

Kertesz M, Iovino N, Unnerstall U, Gaul U, Segal E. The role of site accessibility in microRNA target recognition. Nat Genet. 2007; 39:1278–1284. [PubMed: 17893677]

Komori T, Yagi H, Nomura S, Yamaguchi A, Sasaki K, Deguchi K, Shimizu Y, Bronson RT, Gao YH, Inada M, Sato M, Okamoto R, Kitamura Y, Yoshiki S, Kishimoto T. Targeted disruption of Cbfa1 results in a complete lack of bone formation owing to maturational arrest of osteoblasts. Cell. 1997; 89:755–764. [PubMed: 9182763]

Lee KS, Kim HJ, Li QL, Chi XZ, Ueta C, Komori T, Wozney JM, Kim EG, Choi JY, Ryoo HM, Bae SC. Runx2 is a common target of transforming growth factor beta1 and bone morphogenetic protein 2, and cooperation between Runx2 and Smad5 induces osteoblast-specific gene expression in the pluripotent mesenchymal precursor cell line C2C12. Mol Cell Biol. 2000; 20:8783–8792. [PubMed: 11073979]

Lengner CJ, Hassan MQ, Serra RW, Lepper C, van Wijnen AJ, Stein JL, Lian JB, Stein GS. Nkx3.2-mediated repression of Runx2 promotes chondrogenic differentiation. J Biol Chem. 280:15872–15879. [PubMed: 15703179]

Lian JB, Stein GS, van Wijnen AJ, Stein JL, Hassan MQ, Gaur T, Zhang Y. MicroRNA control of bone formation and homeostasis. Nat Rev Endocrinol. 2012; 8:212–227. [PubMed: 22290358]

Liu AM, Yao TJ, Wang W, Wong KF, Lee NP, Fan ST, Poon RT, Gao C, Luk JM. Circulating miR-15b and miR-130b in serum as potential markers for detecting hepatocellular carcinoma: a retrospective cohort study. BMJ Open. 2012; 2:e000825.

Liu DD, Zhang JC, Zhang Q, Wang SX, Yang MS. TGF-β/BMP signaling pathway is involved in cerium-promoted osteogenic differentiation of mesenchymal stem cells. J Cell Biochem. 2013; 114:1105–1114. [PubMed: 23150386]

Liu Z, Yang D, Xie P, Ren G, Sun G, Zeng X, Sun X. MiR-106b and MiR-15b modulate apoptosis and angiogenesis in myocardial infarction. Cell Physiol Biochem. 2012; 29:851–862. [PubMed: 22613985]

McGee-Lawrence ME, Li X, Bledsoe KL, Wu H, Hawse JR, Subramaniam M, Razidlo DF, Stensgard BA, Stein GS, van Wijnen AJ, Lian JB, Hsu W, Westendorf JJ. Runx2 protein represses Axin2 expression in osteoblasts and is required for craniosynostosis in Axin2-deficient mice. J Biol Chem. 2013; 288:5291–5302. [PubMed: 23300083]

McGee-Lawrence ME, Westendorf JJ. Histone deacetylases in skeletal development and bone mass maintenance. Gene. 2011; 474:1–11. [PubMed: 21185361]

Monroe DG, McGee-Lawrence ME, Oursler MJ, Westendorf JJ. Update on Wnt signaling in bone cell biology and bone disease. Gene. 2012; 492:1–18. [PubMed: 22079544]

Moorthi A, Vimalraj S, Avani C, He Z, Partridge NC, Selvamurugan N. Expression of microRNA-30c and its target genes in human osteoblastic cells by nano-bioglass ceramic-treatment. Int J Biol Macromol. 2013; 56:181–185. [PubMed: 23469762]

Murakami G, Watabe T, Takaoka K, Miyazono K, Imamura T. Cooperative inhibition of bone morphogenetic protein signaling by Smurf1 and inhibitory Smads. Mol Biol Cell. 2003; 14:2809–2817. [PubMed: 12857866]

Nefussi JR, Boy-Lefevre ML, Boulekbache H, Forest N. Mineralization in vitro of matrix formed by osteoblasts isolated by collagenase digestion. Differentiation. 1985; 29:160–168. [PubMed: 2995186]

Niger C, Luciotti MA, Buo AM, Hebert C, Ma V, Stains JP. The regulation of runt-related transcription factor 2 by fibroblast growth factor-2 and connexin43 requires the inositol

polyphosphate/protein kinase Cδ cascade. J Bone Miner Res. 2013; 28:1468–1477. [PubMed: 23322705]

Nishi H, Ono K, Iwanaga Y, Horie T, Nagao K, Takemura G, Kinoshita M, Kuwabara Y, Mori RT, Hasegawa K, Kita T, Kimura T. MicroRNA-15b modulates cellular ATP levels and degenerates mitochondria via Arl2 in neonatal rat cardiac myocytes. J Biol Chem. 2010; 285:4920–4930. [PubMed: 20007690]

O'Hara AJ, Vahrson W, Dittmer DP. Gene alteration and precursor and mature microRNA transcription changes contribute to the miRNA signature of primary effusion lymphoma. Blood. 2008; 111:2347–2353. [PubMed: 18079361]

Pittenger MF, Mackay AM, Beck SC, Jaiswal RK, Douglas R, Mosca JD, Moorman MA, Simonetti DW, Craig S, Marshak DR. Multilineage potential of adult human mesenchymal stem cells. Science. 1999; 284:143–147. [PubMed: 10102814]

Raggatt LJ, Qin L, Tamasi J, Jefcoat SC Jr, Shimizu E, Selvamurugan N, Liew FY, Bevelock L, Feyen JH, Partridge NC. Interleukin-18 is regulated by parathyroid hormone and is required for its bone anabolic actions. J Biol Chem. 2008; 283:6790–6798. [PubMed: 18165223]

Satzger I, Mattern A, Kuettler U, Weinspach D, Voelker B, Kapp A, Gutzmer R. MicroRNA-15b represents an independent prognostic parameter and is correlated with tumor cell proliferation and apoptosis in malignant melanoma. Int J Cancer. 2010; 126:2553–2562. [PubMed: 19830692]

Selvamurugan N, Jefcoat SC, Kwok S, Kowalewski R, Tamasi JA, Partridge NC. Overexpression of Runx2 directed by the matrix metalloproteinase-13 promoter containing the AP-1 and Runx/RD/Cbfa sites alters bone remodeling *in vivo*. J Cell Biochem. 2006; 99:545–557. [PubMed: 16639721]

Selvamurugan N, Kwok S, Vasilov A, Jefcoat SC, Partridge NC. Effects of BMP-2 and pulsed electromagnetic field (PEMF) on rat primary osteoblastic cell proliferation and gene expression. J Orthop Res. 2007; 25:1213–1220. [PubMed: 17503520]

Selvamurugan N, Pulumati MR, Tyson DR, Partridge NC. Parathyroid hormone regulation of the rat collagenase-3 promoter by protein kinase A-dependent transactivation of core binding factor alpha1. J Biol Chem. 2000; 275:5037–5042. [PubMed: 10671545]

Shen R, Chen M, Wang YJ, Kaneki H, Xing L, O'keefe RJ, Chen D. Smad6 interacts with Runx2 and mediates Smad ubiquitin regulatory factor 1-induced Runx2 degradation. J Biol Chem. 2006; 281:3569–3576. [PubMed: 16299379]

Shimizu E, Selvamurugan N, Westendorf JJ, Olson EN, Partridge NC. HDAC4 represses matrix metalloproteinase-13 transcription in osteoblastic cells, and parathyroid hormone controls this repression. J Biol Chem. 2010; 285:9616–9626. [PubMed: 20097749]

Vejnar CE, Blum M, Zdobnov EM. miRmap web: comprehensive microRNA target prediction online. Nucleic Acids Res. 2013; 41:W165–W168. [PubMed: 23716633]

Vejnar CE, Zdobnov EM. MiRmap: comprehensive prediction of microRNA target repression strength. Nucleic Acids Res. 2012; 40:11673–11683. [PubMed: 23034802]

Vimalraj S, Miranda PJ, Ramyakrishna B, Selvamurugan N. Regulation of breast cancer and bone metastasis by microRNAs. Dis Markers. 2013; 35:369–387. [PubMed: 24191129]

Vimalraj S, Selvamurugan N. MicroRNAs: synthesis, gene regulation and osteoblast differentiation. Curr Issues Mol Biol. 2012; 15:7–18. [PubMed: 22581832]

Wang CY, Yang SF, Wang Z, Tan JM, Xing SM, Chen DC, Xu SM, Yuan W. PCAF acetylates Runx2 and promotes osteoblast differentiation. J Bone Miner Metab. 2013

Westendorf JJ, Zaidi SK, Cascino JE, Kahler R, van Wijnen AJ, Lian JB, Yoshida M, Stein GS, Li X. Runx2 (Cbfa1, AML-3) interacts with histone deacetylase 6 and represses the p21(CIP1/WAF1) promoter. Mol Cell Biol. 2002; 22:7982–7992. [PubMed: 12391164]

Wilmink GJ, Roth CL, Ibey BL, Ketchum N, Bernhard J, Cerna CZ, Roach WP. Identification of microRNAs associated with hyperthermia-induced cellular stress response. Cell Stress Chaperones. 2010; 15:1027–1038. [PubMed: 20352393]

Yang S, Xu H, Yu S, Cao H, Fan J, Ge C, Fransceschi RT, Dong HH, Xiao G. Foxo1 mediates insulin-like growth factor 1 (IGF1)/insulin regulation of osteocalcin expression by antagonizing Runx2 in osteoblasts. J Biol Chem. 2011; 286:19149–19158. [PubMed: 21471200]

Zhao L, Huang J, Guo R, Wang Y, Chen D, Xing L. Smurf1 inhibits mesenchymal stem cell proliferation and differentiation into osteoblasts through JunB degradation. J Bone Miner Res. 2010; 25:1246–1256. [PubMed: 20200942]

Zhao M, Qiao M, Harris SE, Oyajobi BO, Mundy GR, Chen D. Smurf1 inhibits osteoblast differentiation and bone formation *in vitro* and *in vivo*. J Biol Chem. 2003; 279:12854–12859. [PubMed: 14701828]

Zhu H, Kavsak P, Abdollah S, Wrana JL, Thomsen GH. A SMAD ubiquitin ligase targets the BMP pathway and affects embryonic pattern formation. Nature. 1999; 400:687–693. [PubMed: 10458166]
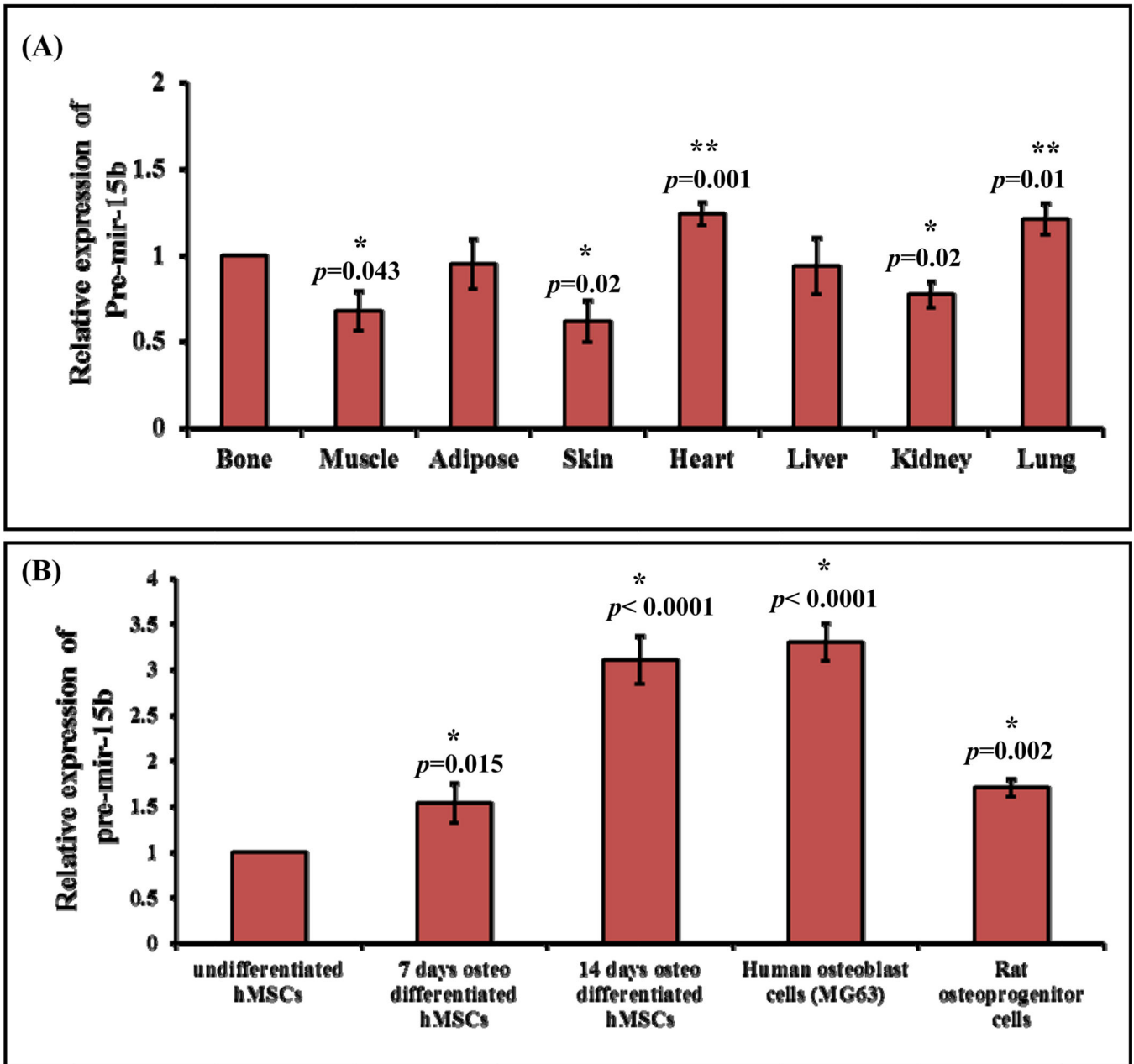
Figure 1.

Expression of stem loop sequences of miR-15b. **(A)** Real time RT-PCR analysis of pre-mir-15b expression in multiple tissues. * represents significant down regulation and ** represents significant up regulation compared to bone tissue. **(B)** Real time RT-PCR analysis of precursor pre-mir-15b expression in undifferentiated hMSCs, 7-days osteo-differentiated hMSCs, 14-days osteo-differentiated hMSCs, human differentiated osteoblast cells, MG63 and rat osteoprogenitor cells. * represents significant up regulation compared to undifferentiated hMSCs.
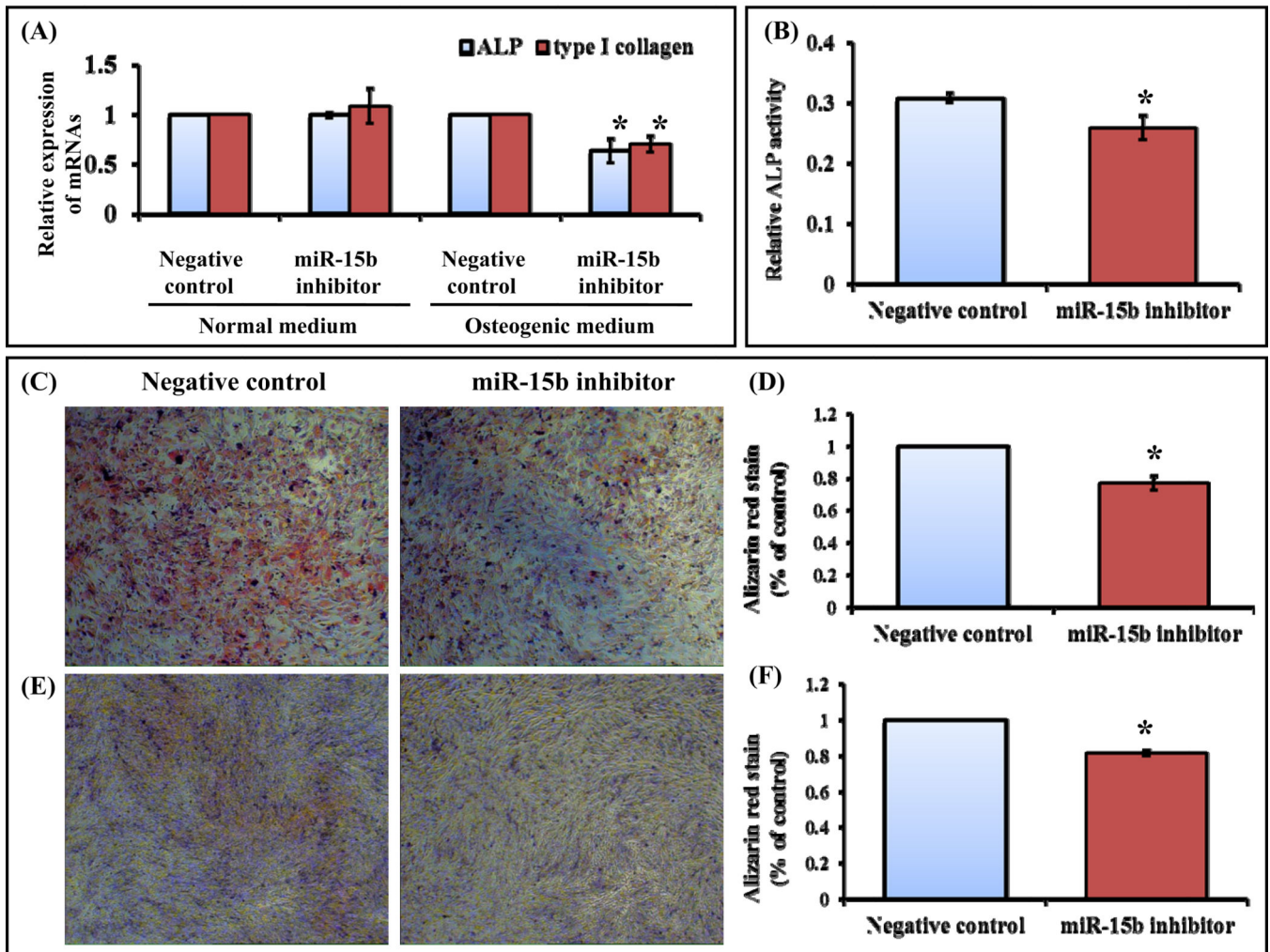
Figure 2.
miR-15b inhibitor down regulates osteoblast differentiation. **(A)** Rat osteoprogenitor cells were transiently transfected with 50 nM of negative control miRNA or miR-15b inhibitor in normal medium or osteogenic medium for 7 days. Total RNA was isolated and real time RT-PCR was carried out using the primers for ALP and type 1 collagen genes. Relative expression of mRNAs was calculated after normalization with GAPDH. **(B)** Mouse MSCs (C3H10T1/2) were transiently transfected with 50 nM of negative control miRNA or miR-15b inhibitor in osteogenic medium for 7 days and the cells were subjected to Alkaline phosphatase activity measurement. **(C)** Alizarin Red staining was performed in 50 nM of miR-15b inhibitor or negative control miRNA transfected C3H10T1/2, mouse MSC cells at days 7 in osteogenic medium. **(D)** The graph showed the quantitative analysis of the mineralized matrix. **(E)** Human osteoblastic cells (MG63) were transiently transfected with 50 nM of negative control miRNA or miR-15b inhibitor in osteogenic medium for 7 days. Cells were stained with Alizarin Red and were visualized for mineralized matrix under microscope. **(F)** Quantitative analysis of the mineralized matrix as shown above. * indicates significant down regulation compared to negative control.
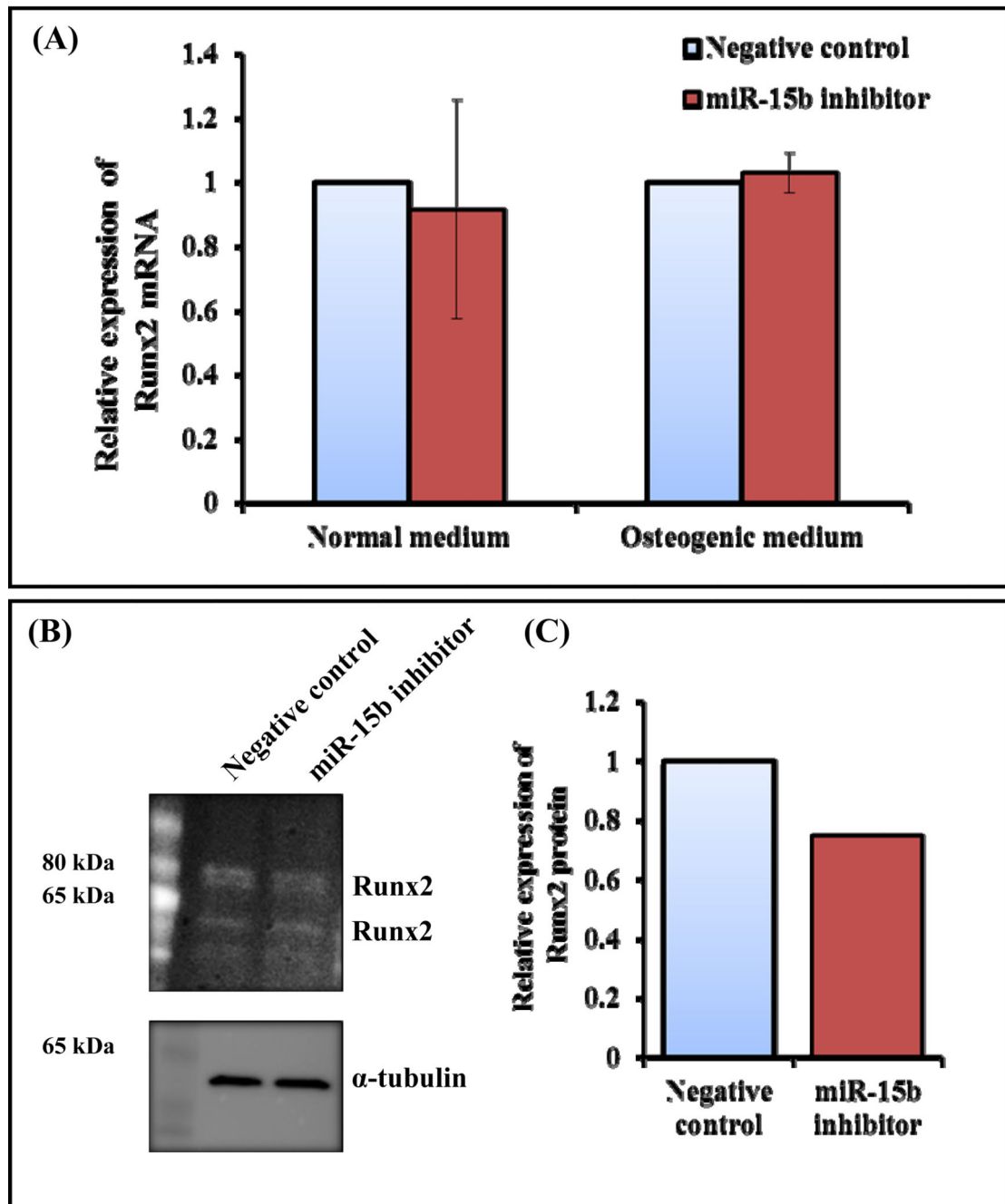
Figure 3.
Regulation of Runx2 by miR-15b inhibitor during hMSCs differentiation towards osteoblasts. hMSCs were transiently transfected with 50 nM of negative control miRNA or miR-15b inhibitor in the presence of normal medium or osteogenic medium. **(A)** At day 10, total RNA was isolated and real time RT-PCR was carried out using the primers for Runx2 and GAPDH genes. Relative expression of Runx2 mRNA was calculated after normalization with GAPDH. **(B)** At day 10, whole cell lysates were prepared and subjected to Western blot analysis using the antibody for Runx2. α-tubulin was used as internal control. **(C)** The

densitometry scanning of the above Western blot after normalization with α-tubulin. The experiment was carried out three times and a representative blot is given.
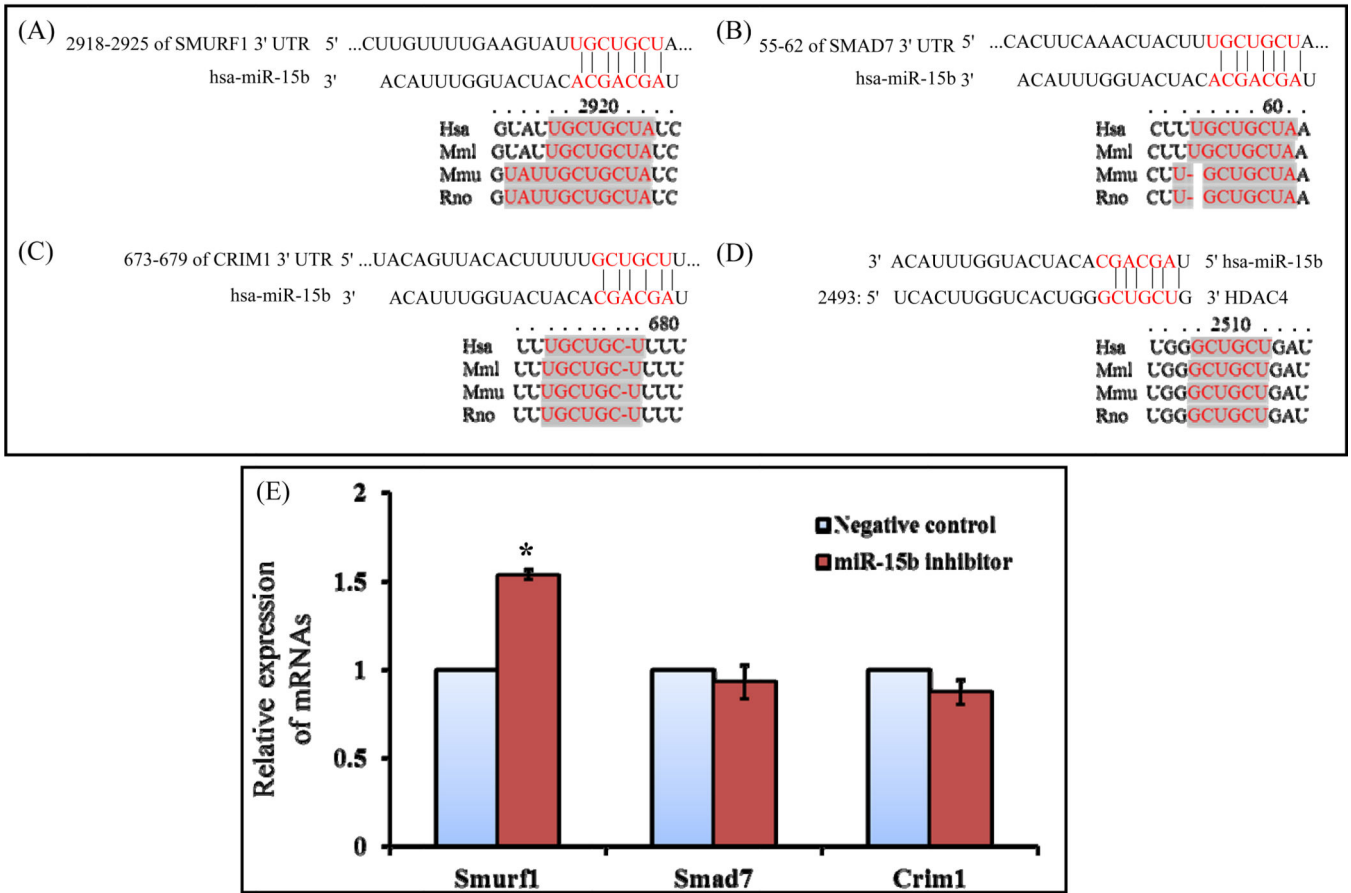
Figure 4.
miR-15b inhibitor up regulates expression of Smurf1 mRNA. The putative target region analysis was performed for Smurf1, Smad7 and Crim1 mRNAs 3' UTR by miR-15b seed sequence. Interspecies conservation or similarity of putative miR-15b binding region was shown in 3'UTR of Smurf1 (**A**), Smad7 (**B**), Crim1 (**C**) and HDAC4 (**D**). The shadow or colored pointed sequence indicate the perfectly conserved sequences between human and other species (**E**) Rat osteoprogenitor cells were transiently transfected with 50 nM of negative control miRNA or miR-15b inhibitor for 7 days in osteogenic medium. Total RNA was isolated and real time RT-PCR was carried out using the primers for Smurf1, Smad7 and Crim1 genes. Relative expression of mRNAs was calculated after normalization with GAPDH. * indicates significant up regulation of mRNA compared to negative control.
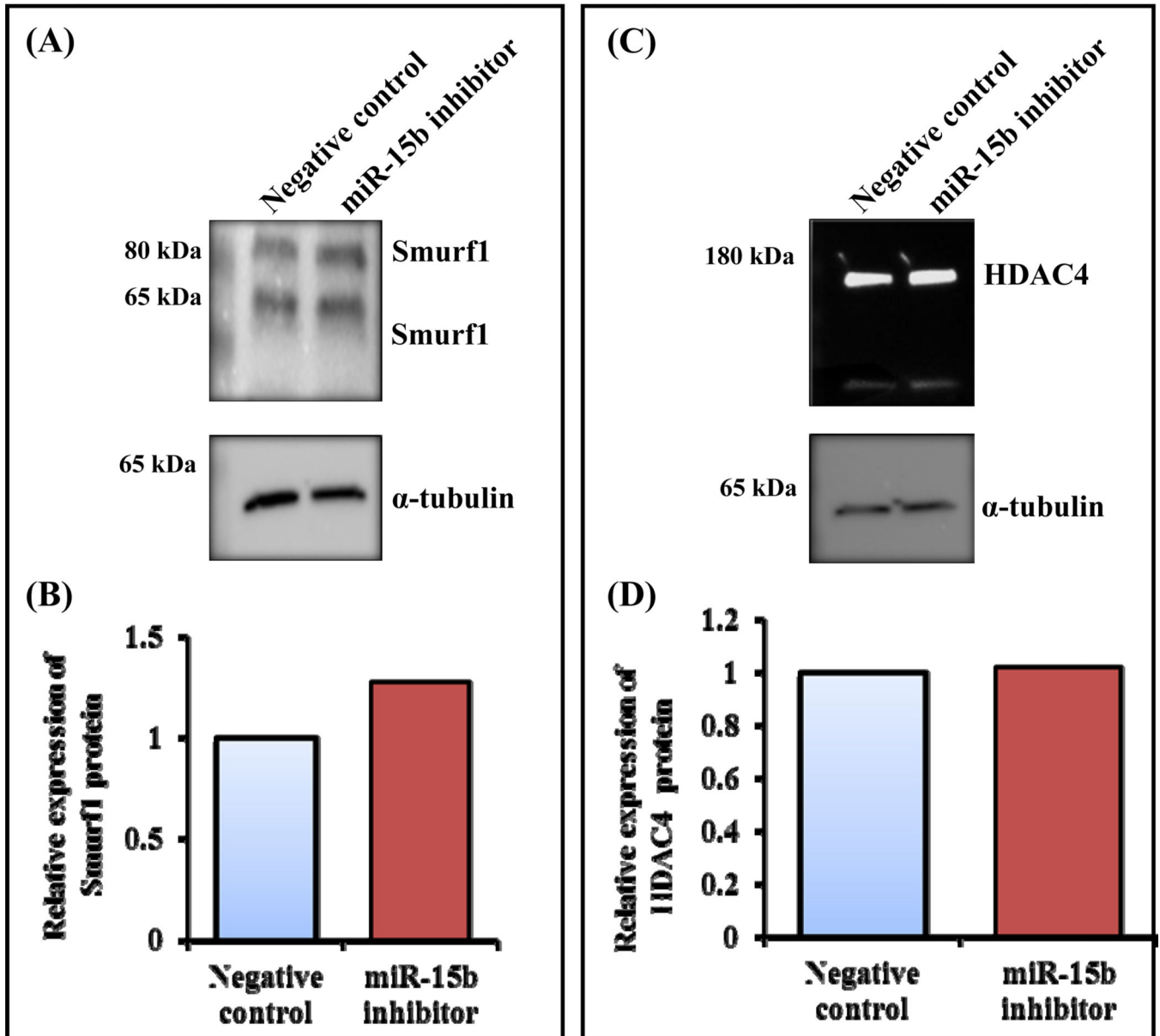
Figure 5.
Translational regulation of miR-15b's putative target genes, Smurf1 and HDAC4. (**A**)
hMSCs were transiently transfected with 50 nM of negative control miRNA or miR-15b
inhibitor in the presence of osteogenic medium. At day 10, whole cell lysates were prepared
and subjected to Western blot analysis using the antibody for Smurf1. α-tubulin was used as
internal control. (**B**) The densitometretic scanning of the above Western blot after
normalization with α-tubulin. (**C**) hMSCs were transiently transfected with 50 nM of
negative control miRNA or miR-15b inhibitor in the presence of osteogenic medium. At day
10, whole cell lysates were prepared and subjected to Western blot analysis using the
antibody for HDAC4. α-tubulin was used as internal control. (**D**) The densitometry scanning

of the above Western blot after normalization with α-tubulin. The experiment was carried out three times and a representative blot is given.
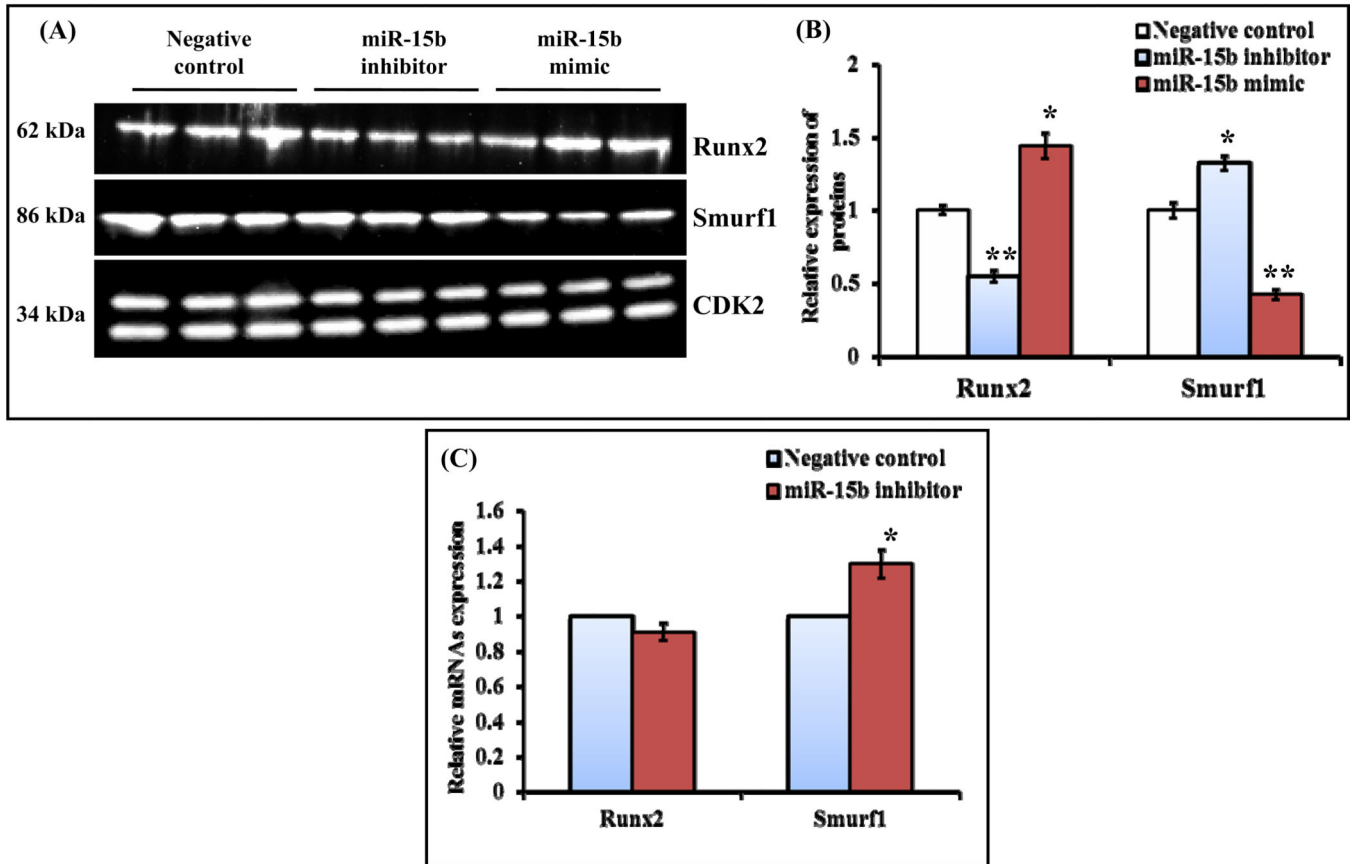
Figure 6.
miR-15b down regulates Smurf1 and up regulates Runx2 proteins expression. **(A)** C3H10T1/2 cells were transiently transfected with 50 nM of negative control miRNA, miR-15b inhibitor or miR-15b mimic. At day 7, whole cell lysates were prepared and subjected to Western blot analysis using the antibodies as indicated. CDK2 was used as internal control. **(B)** Densitometry scanning of these proteins expression by Western blot after normalization with CDK2. * represents significant up regulation and ** represents significant down regulation compared to negative control miRNA. **(C)** At day 7, total RNA isolation and real time RT-PCR analysis were carried out for determination of Runx2 and Smurf1 mRNA expression. U6 served as internal control. The relative expression of Runx2 and Smurf1 was calculated after normalization with U6 expression.
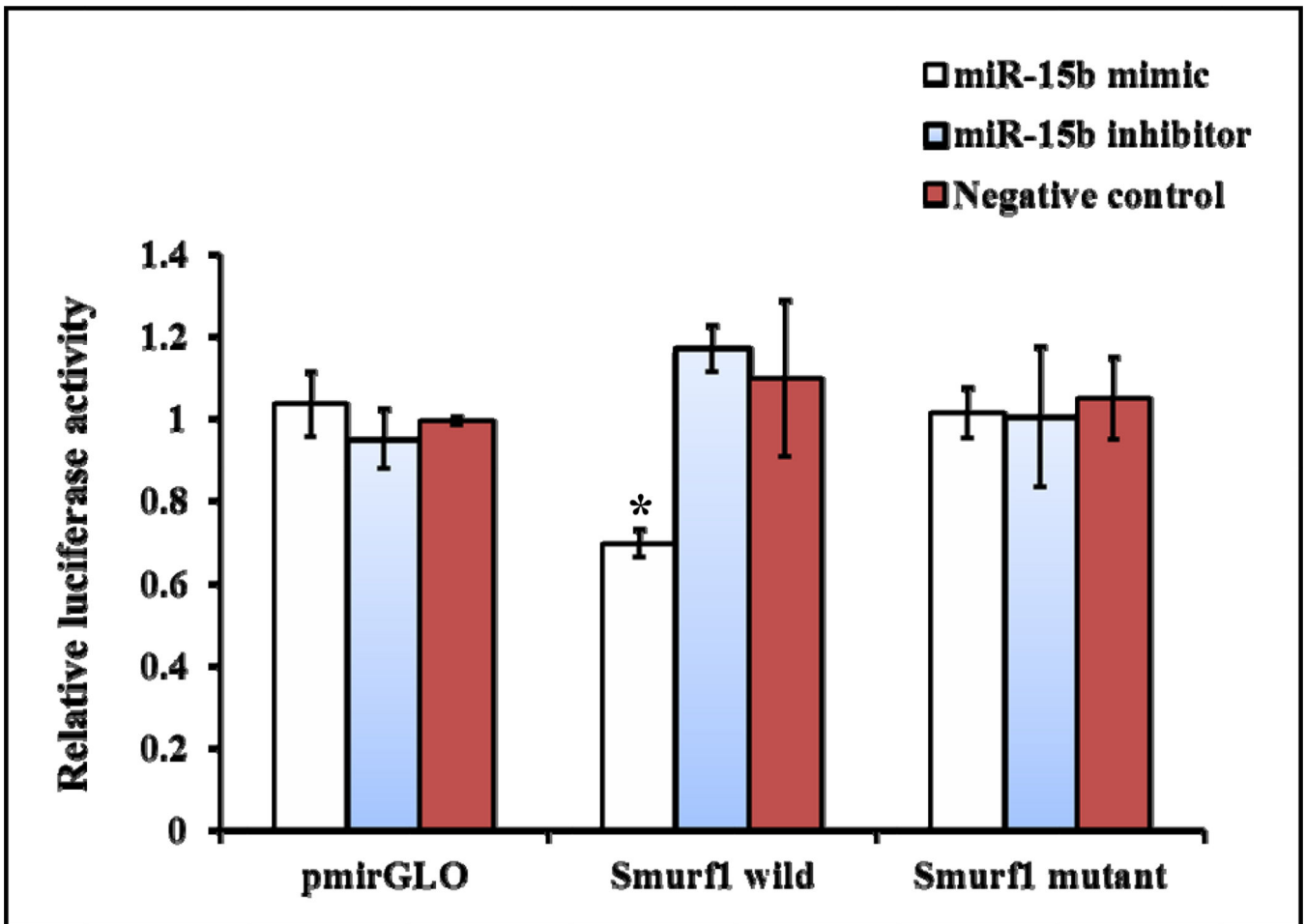
Figure 7.
miR-15b directly targets Smurf1 3'UTR. A part of Smurf1 3'UTR region was predicted to be a target gene of miR-15b (Fig. 4A). The predicted target sequence and its mutated sequence were cloned into a luciferase construct (pmirGLO). C3H10T1/2 cells were transiently transfected with the pmirGLO construct or the pmirGLO construct containing either wild or mutant Smurf1 3'UTR along with miR-15b mimic, inhibitor or negative control miRNA. After 24 hrs, cell lysates were prepared and subjected to determination of relative luciferase activity by normalization of firefly luciferase activity with *Renilla* luciferase activity. * indicates significantly decreased luciferase activity.

Table 1

Primer sequences used for real time RT-PCR.

Name of the genes		Sequence (5'->3')
pre-mir-15b	Forward	GGCCTTAAAGTACTGTAGCAGC
	Reverse	CCTTAAATTTCTAGAGCAGC
U6	Forward	CTCGCTTCGGCAGCACA
	Reverse	AACGCTTCACGAATTTGCGT
Runx2	Forward	GACCAGTCTTACCCCTCCTACC
	Reverse	CTGCCTGGCTCTTCTTACTGAG
ALP	Forward	AGGCAGGATTGACCACGG
	Reverse	TGTAGTTCTGCTCATGGA
Type1 collagen	Forward	TAACCCCCTCCCCAGCCACAAA
	Reverse	TTCCTCTTGGCCGTGCGTCA
Smurf1	Forward	CGGTGGAGACCTTCGATGAG
	Reverse	CAGAGCCTTGAAGCCTTGGA
Smad7	Forward	ACCCGATGGATTTTCTCAAAC
	Reverse	GCCAGATAATTCGTTCCCCC
Crim1	Forward	GCCAACAAGATGCGAGTGTC
	Reverse	AGACTATGCGGGGAGTGGAT
Rat GAPDH	Forward	GCAGAGGTTGAATGTGAGCA
	Reverse	GGAAGAAGTTCCCATCGTCA
Human GAPDH	Forward	TTGATGTCATCATACTTGGCAGGT
	Reverse	CAG TCAAGGCTGAGAATGGGA

Table 2

Putative targets of miR-15b, the free energy predicted by miRmap and PITA algorithm.

Target genes	Sequence	miRmap: Comprehensive prediction of microRNA target repression strength[a]											PITA: Thermodynamic model[b]			TarBase[c] and miRecords[d] validation
		G duplex	G binding	G duplex seed	G binding seed	G open	G total	Probability		Conservation		miRmap score	G duplex	G open	G total	
								exact	binomial	BLS	PhyloP					
Smurf1	NM_020429	−13.40	−13.95	−10.10	−10.71	9.27	−4.13	0.33	0.44	1.49	0.0	−0.23	−15.7	−8.33	−7.36	No
HDAC4	NM_006037	−11.40	−12.91	−8.50	−8.91	32.77	21.37	0.57	0.99	0.11	0.85	0.05	−11.5	−12.97	1.47	No
Smad7	NM_005904	−14.20	−14.91	−10.10	−10.71	20.96	6.76	0.23	0.23	0.79	0.03	−0.22	−15.51	−7.0	−8.5	No
Criml	NM_016441	−11.50	−12.44	−10.10	−10.71	13.72	2.22	0.27	0.23	0.46	0.18	−0.19	−11.7	−6.51	−5.18	No

[a] miRmap: http://mirmap.ezlab.org/

[b] PITA: http://genie.weizmann.ac.il/index.html

[c] TarBase: http://diana.cslab.ece.ntua.gr/DianaToolsNew/index.php?t=tarbase/index

[d] miRecords: http://mirecords.biolead.org/